HT-SMES Operating at Liquid Nitrogen Temperatures for Electric Power Quality Improvement Demonstrating

A. Friedman, N. Shaked, E. Perel, F. Gartzman, M. Sinvani, Y. Wolfus, D. Kottick, J. Furman, and Y. Yeshurun

***Abstract*—We have developed and tested a laboratory scale High-T_C Superconducting Magnetic Energy Storage (HT-SMES) system with storage capacity of up to 1.2 kJ. It was designed to improve the power quality for a consumer supplied by 3-phase standard commercial electric power grid at a consumer power of up to 20 kW. This SMES is based on a high-T_C superconducting coil with a ferromagnetic core, immersed in liquid nitrogen at 65 K to provide efficient thermal contact with the coolant. We also developed a cryogenic DC-DC converter based on low resistance power MOSFET transistors, providing low losses in the stored energy and high operational efficiency. The power conditioning capability of our HT-SMES was proved, and compensation of voltage drops in the electric grid was successfully demonstrated.**

***Index Terms*—Converters, energy storage, high-temperature superconducting magnets, liquid nitrogen cooling, voltage control.**

I. Introduction

THE POWER quality problem is characterized by power interruptions, voltage sags, and frequency modulations with a typical duration in the milliseconds to seconds time regime. In principle, SMES devices offer the right response time for addressing the power quality problem [1]. In the recent years commercial LT-SMES devices have become available [2]. HT-SMES devices are still in their early research and development stages [3]–[6]. Beside the high cost of HTS wires, the strong field dependence of the critical current is an obstacle for achieving high stored energy values. Most of the research groups have therefore turned to operating at the 30 K temperature regime. This temperature regime is achieved by a cryogen free cooling and is a reasonable compromise between the stored energy level and the cooling efficiency and costs. While cryogen free cooling is very appealing, it creates problems of temperature homogeneity across the HTS coil and difficulties in fast removing of the heat generated during the SMES charge and discharge processes.

In a previous study [3], we have selected a different approach. A first demonstration HT-SMES model (120 J, 12 V) was built, cooled with *liquid nitrogen* (LN_2) to be operated in temperatures 65–77 K. In this paper we describe an up scaling of our HT-SMES using basically the same approach. The new laboratory scale model carries currents up to 100 A, stores up to 1.2 kJ energy and supports 20 kW output power. In the following sections we will describe the magnetic and the power circuits of our HT-SMES and the testing procedures that have been performed. To our knowledge, this is the first demonstration of an HT-SMES device operating at LN_2 temperatures.

Manuscript received August, 6, 2002. This work was supported in part by the Ministry of National Infrastructures (IMNI) and the Israel Electric Corporation (IEC).

A. Friedman, N. Shaked, E. Perel, F. Gartzman, M. Sinvani, Y. Wolfus, and Y. Yeshurun are with the Institute of Superconductivity, Bar-Ilan University, Ramat-Gan, 52900, Israel (e-mail: freidma@mail.biu.ac.il).

D. Kottick and J. Furman are with the R&D Electrical Laboratory, the Israel Electric Corp. Ltd., Haifa 31000, Israel.

Digital Object Identifier 10.1109/TASC.2003.812935

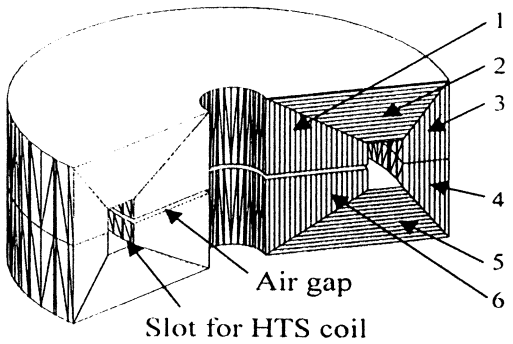

Fig. 1. A scheme of the layered iron core assembled from 6 different parts. The lines seen in the core cross section indicate the direction of the lamination.

II. Superconducting Magnet

The energy-storing unit of the SMES is composed of a HTS coil and a ferromagnetic core. The magnetic fields that produced by BSCCO coils at temperatures of LN are quite small because of the fast decrease in the critical current density with increasing magnetic field. This strong J_C(B) dependence is even more dramatic for fields perpendicular to the tape's plane [7]. The best solution for LN_2-cooled SMES design is the use of a ferromagnetic core that increases the inductance of the coil and thus the stored energy, and at the same time decreases the magnetic field on the winding allowing for higher operating currents. We have found that a "pot-core" configuration provides a good solution having a minimal volume and allowing the control of dissipation fields. The core was assembled out of 6 parts as shown in Fig. 1. This construction allows us to adapt the length of the air gap for maximizing the stored energy at any selected operating temperature. All core components have been manufactured from laminated steel of type STABOLEC grade 230-50 A. The direction of lamination in all parts coincides with the direction of the magnetic field.

The coil was purchased in 1998 from American Superconductor Corporation (ASC) reflecting the state of the art then. Its diameter was determined by the diameter of the standard dewar that had to accommodate the coil and the core. The coil had more

TABLE I
THE COIL AND MAGNETIC CORE PARAMETERS

HTS Coil	Outside diameter, mm	390	
	Inside diameter, mm	370	
	Height, mm	62	
	No. of double pancakes	8	
	No. of turns	256	
	Conductor length, m	300	
	Inductance, H	0.04	
	Operating voltage, V	400	
	Operating temperature	64 K	77 K
	Critical current, A	110	55
	Maximal stored energy, J	240	60
Magnetic core	Outside diameter, mm	530	
	Height, mm	250	
	Cross section area, m^2	0.08	
	Length of air gap, mm	10	19
Coil with core	Maximal stored energy, J	1500	750
	Energy gain	6.25	12.5
	Peak power, kW	44	22
	Average inductance, H	0.29	0.55

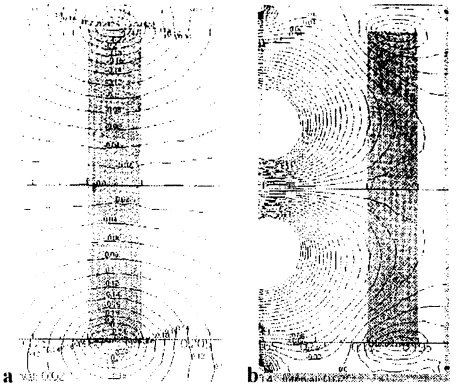

Fig. 2. Distribution of the radial field component BR on the coil winding and (a) its vicinity for the coil without core and (b) for the coil surrounded by the optimized ferromagnetic core.

than 25 000 Ampere-turns to assure the required stored energy. Table I lists the coil parameters. The coil is wound in two identical sub-coils, one on top of the other and electrically connected in series.

The magnetic field generated by the coil is much smaller than the saturation field of iron, therefore enabling a significant increase of the coil stored energy by using the ferromagnetic core. The energy stored in the coil and core setup has a maximum at a specific length of the core's air gap. The internal toroidal space ("window") inside the core for the coil was also optimized for achieving a minimal radial component of the magnetic field on the winding. To refine the geometry of the core we have performed numerical calculations with PC-OPERA software for 2 of Ampere-turns values: 12 500 and 25 000 related to the operation current at temperatures of 77 K and 65 K respectively. We calculated the stored energy in the coil with the core, values of the flux density in the magnetic volume, and the distribution of the radial and axial components on the HTS winding.

Fig. 2 shows the distribution of the radial field component on the winding for a coil without a core and for the coil surrounded

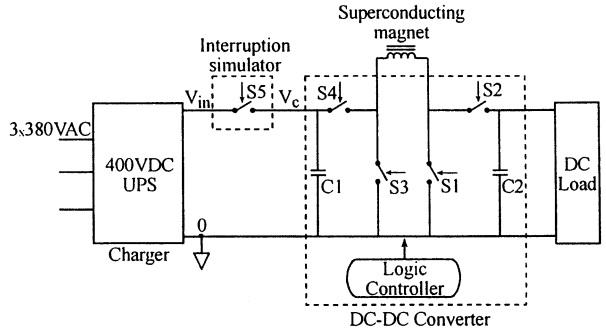

Fig. 3. Outline of the electric circuit of the SMES.

by the optimized ferromagnetic core. In the first case the maximal radial field value reaches 0.27 T on the top and bottom surfaces of the coil. The maximal radial field in the presence of the core drops to less than 0.1 T at all surfaces of the coil achieving maximum on the inner or top (bottom) surfaces. The axial component of the magnetic field increases in the presence of the core from 0.26 T to 0.65 T. However, this increase does not create a problem since the axial component exerts much smaller influence on J_C.

This analysis shows that a proper design of the core 'window' can reduce significantly the magnetic field on the winding thereby reducing the J_C(B) problem, allowing for substantial operating currents at LN_2– temperatures. The parameters of the optimized ferromagnetic core are listed in Table I.

III. ELECTRICAL AND ELECTRONIC CIRCUIT

A crucial component of the electronic circuit of SMES is the DC-DC converter. In order to improve the efficiency of the SMES we have designed a special cryogenic DC-DC converter based on power MOSFET transistors exhibiting low resistance at LN2 temperatures. The resistance of applied MOSFETs ATP6015 drops at LN_2 temperatures to 15 mOhm (about 10 times less than its room temperature resistance). To further decrease the losses in the switches, every switch was built of several transistors connected in parallel.

Switches S1 and S3 include 6 transistors each. The DC-DC converter is designed for 100 A HTS coil current operation. The voltage level is defined by the input and output converters. These were designed for operation in the 250–400 V range. The output power of the SMES was set to 20 kW allowing the use of 75% the stored energy. Special filters and snubbers with recuperation circuits that enable the suppression of spikes and over-voltages without the essential losses, thus protecting the coil and the switching transistors against voltage spikes. To attain maximal reliability, the passive protective elements were designed and installed: bi-directional transorber for a fast response and parallel varistor for high-energy absorbance. The DC-DC converter includes a switching circuit (S1–S4) and a logic control circuit (controller). The switching circuit enables 4 basic states of the SMES: charge, persistence, discharge and transmission. The SMES adjusts the output voltage making it independent of input voltage. The controller allows for manual and remote settings of the main operating SMES parameters, namely the maximal and minimal coil current, the output voltage, the minimal

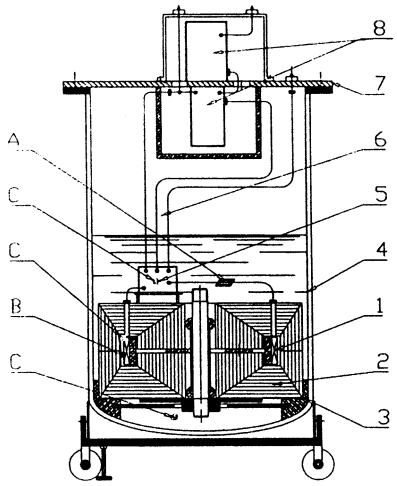

Fig. 4. Layout of the SMES dewar. 1—Superconducting coil, 2—Ferromagnetic core, 3—Core support, 4—Main dewar, 5—Switching circuit, 6—Current leads, 7—Flange, 8—Electronic boxes, A—current probe, B—field probe, C—Thermometers.

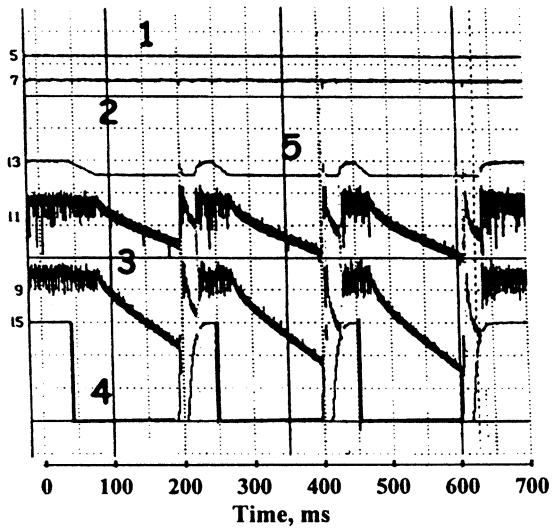

Fig. 5. Demonstration of the SMES operation in a series of sequential DC power interruptions. 1—output voltage, 2—output current, 3—current of the HTS coil, 4—input voltage, 5—voltage on the input capacitor.

input capacitor voltage, and the acceptable ripple at the maximal coil current and at the output voltage. For avoiding design and production of standard devices as rectifier and DC-AC inverter we used the suitable units of industrial UPS (10 kVA).

IV. System Integration and Measurements

The main components of the SMES system and the measuring probes are schematically shown in Fig. 4. The superconducting coil 1) is mounted inside the ferromagnetic core 2) placed upon a support of polyethylene on the bottom of the dewar 4). The coil is supported by right-angle profiles that ensure the required space between the coil and the core. Similarly, the plastic spacers ensure the required air gap between the core parts. The switching circuit 5) is mounted on the upper surface of the iron core near the coil to minimize the resistance of the energy storing circuit. Components 1–5 are all immersed in LN_2.

Current leads shown here represent the input, output, and ground lines to the boxes 8) installed on the dewar cover 7). These boxes include large input and output electrolytic capacitors and varistors that cannot operate at the temperatures below $-50\,^{\circ}$C. The upper box includes drivers and power supply cards. All electrical cables, including power, control and measurement lines pass through these boxes. The dewar cover and the upper box are hermetically sealed to allow for pumping the internal volume of the dewar. The location of thermometers, current and magnetic field probes also is shown (A–C).

Operation of the SMES for compensation of the power supply interruptions was tested in collaboration with the Israel Electric Company (IEC) research team. During the test, a multi-channel recorder registered the mentioned above probes of the SMES as well as input and output voltage and current. For the simulation of voltage interruptions we used a programmable power supply with maximal power 2.5 kW. The test included a single interruption of the input power as well as a series of successive interruptions with maximal duration of 1 s. The test also included partial interruptions i.e., partial drop in voltage of 20 and 50%. The main purpose was to verify that the SMES compensates for

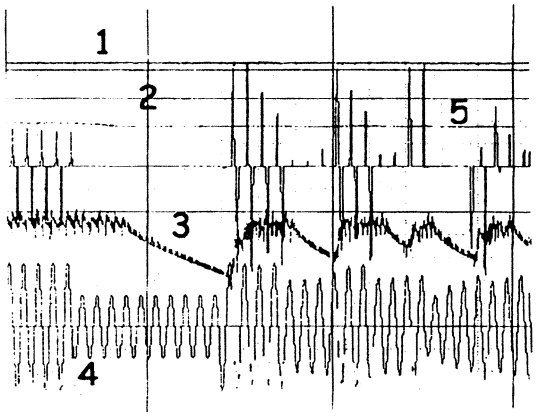

Fig. 6. Demonstration of the SMES operation in a single interruption of the AC power. The input voltage drops to 50%. 1—output voltage, 2—output current, 3—current of the HTS coil, 4—input voltage, 5—voltage on the input capacitor.

input voltage drops, i.e., the load voltage is maintained stable under the various interruptions in power supply.

Fig. 5 shows a sequence of 3 input voltage interruptions. At the moment of interruption switch S5 disconnects the input capacitor C1 from the power supply (see Fig. 3) and its charge is stopped. During the first 20 ms of the interruption, the output power was supplied by the capacitor C3. When its voltage reached the preset minimum level, the discharge of the capacitor is stopped and then the superconducting coil begins to discharge, supplying its energy to the load. Every interruption lasted for 150 ms. To prevent an overload of the power supply, the rate of the input voltage increase and the input current were limited at the end of the interruption. Actually, the input voltage returned to the nominal level within $\sim$20 ms. When the input voltage level reached the minimal voltage of the input capacitor, the charging process resumed and the coil current rose quickly to its initial level. As seen in Fig. 5, the load voltage is kept constant during the entire interruptions period.

The second series of tests was performed with AC power supply interruptions. Figs. 6 and 7 show behavior of the system

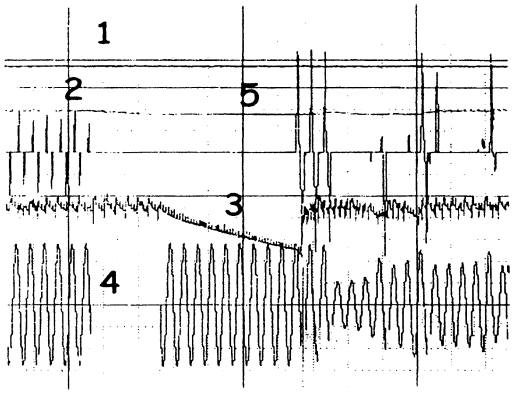

Fig. 7. Behavior of the SMES during the full input voltage drops of AC power. 1—output voltage, 2—output current, 3—current of the HTS coil, 4—voltage on the input capacitor, 5—input voltage.

during full interruption (Fig. 6) and when input voltage drops to 50% of the nominal voltage (Fig. 7). In both tests the SMES successfully supports the constant output voltage. At the recovery stage the power supply is overloaded and its operation become unstable. One can see that SMES helps to power supply to overcome this unstable state. These tests demonstrated application of the HT-SMES for compensation voltage drops and power supply instability.

V. Summary

We have designed and built a laboratory scale SMES device based on HTS coil (HT-SMES) to demonstrate the improving electric power quality in an industrial load. We found some practical solutions for the improvement of the liquid nitrogen operated SMES performances despite the J_C(B) limitation. These solutions include: i) specially designed ferromagnetic core that increases the stored energy by a factor of more than 5 and, at the same time, decreases the perpendicular field component on the windings, ii) decreasing the temperature of the LN_2 from 77 K to 64 K for additional doubling of the stored energy, iii) a unique dc-dc converter immersed in the LN_2 for improved SMES efficiency. These solutions were implemented in the SMES device with a storing capacity of up to 1.2 kJ at 64 K supplied from standard three phase 3×380 V grid.

Acknowledgment

The authors thank Y. Milshtein and A. Einav (IMNI) and D. Viner, G. Meron, O. Kogel, E. Yogev, and E. Hanan (IEC) for their continuous interest in this work, and L. Musafi (IEC) for the help in the tests.

References

[1] R. F. Giese, *Progress Toward High Temperature Superconducting Magnetic Energy Storage (SMES) Systems—A Second Look*. Argonne, IL: Argonne National Laboratory, 1998.

[2] J. B. Howe, "Distributed SMES: A new technology supporting active grid management," *Electrical Line*, Jan./Feb. 2001.

[3] A. Friedman, N. Shaked, E. Perel, M. Sinvani, Y. Wolfus, and Y. Yeshurun, "Superconducting magnetic energy storage device operating at liquid nitrogen temperatures," *Cryogenics*, vol. 39, no. 53, 1999.

[4] S. S. Kalsi, D. Aized, B. Connor, G. Snitchler, J. Campbell, R. E. Schwall, J. Kellers, T. Stephanblome, and A. Tromm, *IEEE Trans. ASC*, vol. 7, p. 971, 1997.

[5] R. Mikkonen, J. Lehtonen, and J. Paasi, "Philosophy of a quench: Two case studies—LTS wiggler magnet and HTS mu-SMES," *IEEE Trans. ASC*, vol. 9, no. 2, pp. 596–599, June 1999.

[6] R. Kreutz, H. Salbert, D. Krischel, A. Hobl, C. Radermacher, and R. Bussjager, "Hochtemperatur-supraleitender magnetischer Energiespeicher—Design und Demonstratoraufbau," in *Supraleitung und Tieftemperaturtechnik, Tagungsband zum 7 Statusseminar*: Garmisch-Partenkirchen, Dec. 2000, vol. 14./15. See also the paper of this Conference.

[7] J. P. Voccio, A. J. Rodenbush, C. H. Joshi, J. W. Ekin, and S. L. Bray, "The effect of magnetic field orientation on the critical current of HTS conductor and coils," *IEEE Transactions ASC*, pt. 2, vol. 5, no. 2, pp. 1822–1825, June 1995.